Atmos. Chem. Phys., 24, 8737–8750, 2024
https://doi.org/10.5194/acp-24-8737-2024

Atmospheric Chemistry and Physics
Open Access
EGU

Measurement report: Impact of emission control measures on environmental persistent free radicals and reactive oxygen species – a short-term case study in Beijing

Yuanyuan Qin[1], Xinghua Zhang[2], Wei Huang[3], Juanjuan Qin[1], Xiaoyu Hu[1], Yuxuan Cao[1], Tianyi Zhao[1,5], Yang Zhang[1,6], Jihua Tan[1], Ziyin Zhang[4], Xinming Wang[5], and Zhenzhen Wang[7]

[1]College of Resources and Environment, University of Chinese Academy of Sciences, Beijing, 100049, China
[2]Sinopec (Dalian) Research Institute of Petroleum and Petrochemicals Co., Ltd, Dalian, 116045, China
[3]Institute of Environmental Reference Materials of Environmental Development Centre of Ministry of Ecology and Environment, Beijing, 100029, China
[4]Institute of Urban Meteorology, China Meteorological Administration, Beijing, 100089, China
[5]Guangzhou Institute of Geochemistry, Chinese Academy of Sciences, Guangzhou, 510640, China
[6]Beijing Yanshan Earth Critical Zone National Research Station, Beijing, 101408, China
[7]School of Environmental Engineering, Changsha Environmental Protection Vocational College, Changsha, 410004, China

Correspondence: Yang Zhang (zhangyang@ucas.ac.cn) and Jihua Tan (tanjh@ucas.ac.cn)

Received: 15 November 2023 – Discussion started: 2 January 2024
Revised: 27 April 2024 – Accepted: 4 June 2024 – Published: 8 August 2024

Abstract. A series of emission control measures implemented by the Chinese government have effectively reduced air pollution by multiple pollutants in many regions of the country in recent decades. However, the impacts of these control measures on environmental persistent free radicals (EPFRs) and reactive oxygen species (ROSs), the two groups of chemical species that are known to be linked with adverse human health effects, are still not clear. In this study, we investigated the levels, patterns, and sources of EPFRs and gas- and particle-phase ROSs (referred to as G-ROSs and P-ROSs, respectively) in Beijing during the 2015 China Victory Day Parade period when short-term air quality control measures were imposed. EPFRs in the non-control period (NCP) tended to be radicals centered on a mixture of carbon and oxygen, while those in the control period (CP) were mainly oxygen-centered free radicals. The contribution of G-ROSs to the atmospheric oxidizing capacity increased, and that of P-ROSs decreased during the CP compared to the NCP. The strict control measures reduced ambient EPFRs, G-ROSs, and P-ROSs by 18.3 %, 24.1 %, and 46.9 %, respectively; these amounts were smaller than the decreases in most other measured pollutants. Although particle-matter-based air quality control measures have performed well in achieving "Parade Blue", it is difficult to simultaneously reduce the negative impacts of the atmosphere on human health. The Parade Blue days were largely attributed to the dramatic reduction in secondary aerosols, which were also largely responsible for EPFR and ROS reductions. Compared to the cases during the NCP, the source-sector-based concentrations of $PM_{2.5}$, EPFRs, G-ROSs, and P-ROSs during the CP were reduced by 78.7 %–80.8 % when coming from secondary aerosols, by 59.3 %–65.0 % when coming from dust sources, by 65.3 %–67.0 % when coming from industrial emissions, and by 32.6 %–43.8 % when coming from vehicle emissions, while concentrations from other sources increased by 1.61 %–71.5 %. Vehicle emissions and other sources may play complex roles in air quality and public health. This insight will prompt policymakers to reevaluate current air quality management strategies to more effectively address the challenges posed by pollutants such as EPFRs and ROSs.

1 Introduction

Free radicals are atoms or molecules that contain at least one unpaired electron, which enables free radicals to be highly reactive (Khan et al., 2018). Free radicals attached to particles with a lifetime of several days or longer are defined as environmental persistent free radicals (EPFRs, e.g., phenoxy and semiquinone free radicals) to distinguish them from traditional free radicals with a shorter lifetime (Li et al., 2022). The excessive lifetime of EPFRs will lead to a greater risk of human exposure to this group of chemical pollutants (Vejerano et al., 2018). It was estimated that human exposure to EPFRs in Beijing is equivalent to approximately 33 cigarettes containing tar EPFRs being inhaled per day (Xu et al., 2020). Numerous toxicological studies have shown that inhalation of EPFRs is linked to a variety of diseases, such as chronic lung disease and respiratory dysfunction, and thus has detrimental effects on human health (Chen et al., 2019b; Thevenot et al., 2013; Vejerano et al., 2018).

Previous studies have shown that the concentrations of EPFRs in atmospheric particles vary from 1.60×10^{13} to 8.97×10^{15} spins m^{-3} (Wang et al., 2022; Li et al., 2022). EPFRs are primarily derived from incomplete combustion sources such as vehicle exhausts, biomass burning, and coal combustion (Y. Wang et al., 2019; Dugas et al., 2016; Saravia et al., 2013). EPFRs can be formed and stabilized on the surface of particulate matter containing transition metals and substituted aromatic structures that are emitted during combustion processes (Odinga et al., 2020; Chen et al., 2019a). For example, the incomplete combustion of vehicle emissions may be an important source of EPFRs in $PM_{2.5}$ from Xi'an, China (Chen et al., 2018b). Dellinger et al. (2001) demonstrated that EPFRs in $PM_{2.5}$ in the United States are associated with combustion sources. Fang et al. (2023) reported that high concentrations of EPFRs are emitted from biomass burning. In addition to the combustion sources, EPFRs can also result from secondary processes in the atmosphere. It has been reported that EPFRs can be formed from the heterogeneous reaction of ozone (O_3) and polycyclic aromatic compounds (Borrowman et al., 2016), as well as from the photolysis of polycyclic aromatic hydrocarbons (PAHs) (Li et al., 2022). Moreover, a recent study showed that EPFRs may also be derived from dust sources (Li et al., 2023). Chen et al. (2018a) found that dust storms can increase the concentration of EPFRs in $PM_{2.5}$ and that metal oxides contained within dust particles provide the prerequisite conditions for EPFRs formation. Notably, EPFRs have received widespread attention in recent years because of their ability to convert O_2 molecules into reactive oxygen species (ROSs) (Gehling et al., 2014). However, the sources and formation processes of EPFRs and ROSs and the relationship between these two groups of pollutants are poorly understood, resulting in greater uncertainties in environmental risk assessments.

ROSs are oxygen molecules that contain at least one unpaired electron, including singlet oxygen, superoxide radicals ($^{\bullet}O_2^-$), hydroxyl radicals ($OH^{\bullet}$), hydrogen peroxide (H_2O_2), and organic radicals (Tong et al., 2018; Arangio et al., 2016). Multiple sources of ROSs have been identified, including wood combustion (Zhou et al., 2018), vehicle exhausts (Verma et al., 2010), and cooking emissions (L. Wang et al., 2020). In addition, many studies have demonstrated that secondary sources related to photochemical reactions and oxidation reactions may be important sources of ROSs (Wang et al., 2012). For example, volatile organic compounds (VOCs) and NO_x have been shown to generate ROSs through photochemical reactions (Venkatachari et al., 2007). ROSs can also form on the surface of particles or in the air through reactions with O_3 under dark conditions (Zhu et al., 2018). Further studies showed that $OH^{\bullet}$ and organic radicals can be formed from secondary organic aerosols (SOAs) generated by isoprene and β-pinene, whereas H_2O_2 and $^{\bullet}O_2^-$ are mainly associated with naphthalene SOAs (Tong et al., 2018; Wei et al., 2021). These ROSs play an active role in the atmospheric environment and determine the oxygenation of atmospheric aerosols. More importantly, ROSs can cause oxidative stress, resulting in particle-related health effects (W. Huang et al., 2018). Oxidative stress, referred to as a state of disequilibrium between oxidizing agents (ROSs) and antioxidant defense capacity, has been recognized as a major contributor to organism diseases (Fang et al., 2017). Thus, investigating the variations in the levels and sources of ROSs is vital for understanding the mechanism of ROS formation and the effect of ROSs on human health.

To mitigate air pollution and associated adverse health effects, the Chinese State Council issued a series of air quality control plans in 2013, termed the "Action Plan on Prevention and Control of Air Pollution", which tremendously reduced the concentration of air pollutants in the following decade (J. Huang et al., 2018; Niu et al., 2022). In addition, the Chinese government has implemented stricter short-term control measures to ensure excellent air quality during certain special periods such as when hosting mega-events (S. Wang et al., 2019; Schleicher et al., 2012). In September 2015, the China Victory Day Parade was held in Beijing, and different levels of short-term emission measures were implemented in Beijing and the surrounding cities (Ma et al., 2020). Particle concentrations in Beijing were substantially reduced during this period, achieving the so-called Parade Blue (W. Huang et al., 2018). Other air pollutants, such as primary organic aerosols (POAs), SOAs, water-soluble ions, and gaseous pollutants, also decreased significantly during this period (Zhao et al., 2017; Wang et al., 2017), demonstrating the potential of short-term control measures for reducing air pollution. However, the potential impacts of these measures on

public health, especially regarding EPFRs and ROSs, remain unclear. This event also provided an excellent opportunity to quantify the effectiveness of control measures on EPFRs and ROSs.

In this work, we evaluated the temporal variations in the chemical compositions of $PM_{2.5}$ and gas pollutants during the period when the 2015 China Victory Day Parade was held in Beijing, aiming to explore the influence of short-term air quality control measures on EPFRs, gas-phase ROSs (G-ROSs), and particle-phase ROS (P-ROSs). Additionally, the sources and formation mechanisms of EPFRs, G-ROSs, and P-ROSs were explored using correlation analysis and a positive matrix factorization (PMF) model. The findings from this study have great implications for further understanding the sources and environmental risks of these chemical species and for the development of optimal air pollution control measures.

2 Methods and materials

2.1 Sample collection

All sampling was conducted on the rooftop of a five-floor building at the Institute of Remote Sensing and Digital Earth, Chinese Academy of Sciences (40.01° N, 117.39° E), which is located between the fourth- and fifth-ring roads in the northern Chaoyang District, Beijing, China, and is surrounded by residential buildings and Olympic Forest Park. A total of 76 $PM_{2.5}$ samples, including 38 daytime (08:00–20:00 LT) and 38 nighttime (20:00–08:00 LT the next day) samples, were collected on prebaked quartz filters using a DIGITEL high-flow sampler (DHA-80, DIGITEL, Switzerland), with a flow rate of 500 L min^{-1}, from 13 August to 19 September 2015. The samples were wrapped in aluminum foil and then stored in a refrigerator at −20 °C until analysis. Real-time SO_2, NO_2, and O_3 concentrations were simultaneously monitored online by an SO_2 analyzer (Model 43i, Thermo Scientific, USA), an NO_x analyzer (Model 42i, Thermo Scientific, USA), and an ozone analyzer (Model 49i, Thermo Scientific, USA), respectively.

The specific sample information is shown in Table S1 in the Supplement. The whole sampling period is divided into four sub-periods for analysis, with the specific control measures for each sub-period presented in Table S2. Period 1 (13–19 August) and period 4 (4–19 September) had no control measures implemented (referred to as the non-control period, NCP), period 2 (20–31 August) had regular control measures, period 3 (1–3 September) had stricter control measures, and periods 2 and 3 were defined as the control period (CP).

2.2 Chemical analyses

Organic carbon (OC) and elemental carbon (EC) in $PM_{2.5}$ were measured by a thermal/optical carbon analyzer (model RT-4, Sunset Laboratory Inc., USA). Water-soluble ions (NO_3^-, SO_4^{2-}, Cl^-, NH_4^+, Na^+, K^+, Ca^{2+}, and Mg^{2+}) were analyzed by an ion chromatography analyzer (model ICS-1100, Thermo Scientific, USA). Elements (Li, Na, Mg, Al, K, Ca, V, Mn, Fe, Co, Cu, Zn, As, Se, Rb, Cd, Pb, and Bi) in $PM_{2.5}$ were extracted by microwave digestion with 7 mL of ultrapure water, 2 mL of HNO_3, and 1 mL of H_2O_2, and the concentrations of elements were detected using inductively coupled plasma mass spectrometry (ICP-MS). PAHs were extracted by a liquid mixture of dichloromethane and methyl alcohol and were measured using gas chromatography equipped with a mass selective detector (Agilent 6890/5973 GC/MSD).

2.3 EPFR analyses

A 28 × 5 mm sample filter was cut and placed in an electronic paramagnetic resonance (EPR) spectrometer (EMX-plus, Bruker, Germany) to determine the concentrations of EPFRs. The measurement parameters of the EPR spectrometer were set as follows: the magnetic field strength was 3300–3450 G, the scanning time was 60 s, the microwave power was 8.0 mW, and the modulation amplitude was 2 G. The absolute spin amount and g factor were calibrated with Mg^{2+} and Cr^{3+} standards. Both of these standards have been proven to be effective for calibrating the g factor and absolute spin number of EPFRs (Chen et al., 2019a, b). During the calibration process, the Mg^{2+} and Cr^{3+} standard samples were inserted into the resonator, and the system was tuned. The field offset was set to zero to ensure that the signal measured by the instrument exactly matched the signals for Mg^{2+} and Cr^{3+}. The total spin numbers were divided by the volume of the samples, such that the concentration of EPFRs was expressed as spins per cubic meter (spins m^{-3}). The crucial parameters for characterizing the type and abundance of EPFRs, such as the g factor and line width (ΔH_{p-p}), were extracted from the EPR spectrum. EPFRs with g factors of less than 2.003 are attributed to carbon-centered free radicals, such as cyclopentadienyl radicals, while EPFRs with g factors of 2.004 and above are designated as oxygen-centered free radicals, such as semiquinone radicals (Zhu et al., 2019). Notably, semiquinone radicals have a resonance structure and can have an unpaired electron on the carbon atom. EPFRs with g factors in the range of 2.003–2.004 suggested the existence of complex radicals centered on a mixture of carbon and oxygen or carbon-centered radicals containing oxygen atoms, such as phenoxy radicals (Yang et al., 2017; Hu et al., 2022).

2.4 G-ROS and P-ROS measurements

A gas and aerosol collector–ROS (GAC-ROS) online monitoring system was used to measure the concentrations of G-ROSs and P-ROSs. The theory and constitutions of the GAC-ROS were described in detail by Huang et al. (2016).

In brief, GAC-ROS consists of a sampling section, a reaction and transportation section, and a detection section. Firstly, aerosols with aerodynamic diameters larger than 2.5 µm were removed by a cyclone separator, gas was collected on the water film on the surface of the continuously rotating diffusion tube of the GAC, and $PM_{2.5}$ was trapped by supersaturated water vapor at a certain temperature. Secondly, solutions containing gas and particle samples were reacted with, respectively, 2′,7′-dichlorofluorescin (DCFH) in the presence of horseradish peroxidase (HRP) in two glass reactors. The DCFH method has the lowest specificity and selectivity for different types of ROSs and is capable of reacting with multiple ROSs, including H_2O_2, as well as other short-lived ROSs, such as $OH^{\bullet}$, $^{\bullet}O_2^-$, peroxyl radicals, and peroxynitrite (Bates et al., 2019). Finally, a fluorescence detector was used to measure the concentrations of G-ROSs and P-ROSs. For data accuracy, fresh DCFH and HRP were prepared at least every two days, and H_2O_2 standard curves were created daily.

2.5 Source apportionment

Researchers have successfully employed PMF for the source apportionment of EPFRs and ROSs (Ainur et al., 2023; Y. Wang et al., 2019). In this study, we used the Environmental Protection Agency (EPA) PMF 5.0 version to perform the source apportionment of $PM_{2.5}$, EPFRs, G-ROSs, and P-ROSs. The fundamental principle of PMF involves first calculating the errors of various chemical components in particulate matter using weights, followed by utilizing the least-squares method to estimate the main pollution sources of the particulate matter and their contributions. The PMF model decomposes a matrix of specific sample data (**X**) into a source contribution matrix (**G**) and factor profile matrix (**F**), as well as a residual matrix (**E**), as shown in the following equation:

$$\mathbf{X}_{ij} = \sum_{k=1}^{p} g_{ik} f_{kj} + e_{ij}, \quad (1)$$

where X_{ij} denotes the concentration of the jth species in the ith sample, g_{ik} represents the source contribution of the kth factor to the ith sample, f_{kj} is the factor profile of the jth species in the kth factor, and e_{ij} is the residual matrix.

$PM_{2.5}$, EPFRs, G-ROSs, P-ROSs, OC, EC, water-soluble ions (NO_3^-, SO_4^{2-}, Cl^-, NH_4^+, Na^+, K^+, Ca^{2+}, and Mg^{2+}), and elements (Na, Mg, Al, K, Ca, V, Mn, Fe, Co, Cu, Zn, As, Se, Rb, Cd, Pb, and Bi) were included in the PMF model, with a total sample number of 76. The procedure for the PMF model has been described in many previous reports (Y. Wang et al., 2019; Sharma et al., 2016). Missing concentration values were replaced with "-999". The component concentration was changed to half of the method detection limit (MDL) when it was lower than the MDL. The calculation formula of uncertainty is uncertainty $= K \times C$, where K is the analytical uncertainty, and C represents the concentrations of the chemical components. The quality of the data was evaluated according to the signal-to-noise ratio (S/N), and species with S/N ranging from 1 to 10 were categorized as "strong", while those with S/N ranging from 0.5 to 1 were categorized as "weak". The tracer species were also categorized as "strong". The degree of rotation in the model results was controlled by the FPEAK and FKEY values.

3 Results and discussion

3.1 Temporal variations in air pollution

To investigate the effectiveness of short-term air quality control measures on pollutant concentrations during the 2015 China Victory Day Parade, temporal variations in $PM_{2.5}$, EC, middle-molar-weight PAHs (MMW-PAHs, four-ring PAHs), elements, and gas pollutants were first examined. As shown in Fig. 1, $PM_{2.5}$ concentration decreased continuously from period 1 to period 3 before rebounding in period 4, with the average $PM_{2.5}$ concentration being $\sim 60\,\%$ lower in the CP (periods 2 and 3) than in the NCP (periods 1 and 4). Similarly, EC, a typical marker of fossil fuel combustion (Zhang et al., 2015; Y. Wang et al., 2020), was also $\sim 57\,\%$ lower in the CP than in the NCP, demonstrating that provisional control measures have significantly reduced fossil fuel combustion emissions. Additionally, a 32 % lower MMW-PAH concentration in the CP than in the NCP implied that the control measures were also effective in reducing emissions from diesel vehicle exhausts (Perrone et al., 2014). The concentrations of elements also decreased dramatically, with a 51.4 % lower concentration in the CP than in the NCP.

Regarding the gaseous pollutants, the concentrations of O_3, SO_2, and NO_2 decreased by 10.8 %, 51.2 %, and 45.5 %, respectively, during the CP compared to those in the NCP. NO_2 is mainly derived from vehicle exhaust emissions, and SO_2 is mainly derived from fossil fuel (e.g., coal) combustion (Hien et al., 2014; Ma et al., 2020). Apparently, the control measures implemented during the CP have effectively reduced emissions from industrial coal combustion and vehicle exhausts, both of which are important combustion sources. In contrast, the reduction in O_3 during the CP was much less than that of NO_2, which can be explained by the reduction in the titration reaction between O_3 and NO due to the reduced NO emission from vehicle exhausts (Guo et al., 2016; Okuda et al., 2011). These results showed that the percentage decrease in gaseous pollutants was smaller than that in $PM_{2.5}$.

Different diurnal variations were observed between the pollutants. The average concentrations of EC and NO_2 were generally higher during the nighttime (1.33 µg m^{-3} and 40.2 µg m^{-3}, respectively) than during the daytime (0.82 µg m^{-3} and 28.4 µg m^{-3}, respectively) in the whole measurement period. This is especially the case during the NCP, likely due to increased nighttime traffic emissions or the occurrence of temperature inversions (Yang et al., 2015; Wu et al., 2012). During the daytime, the restrictions on heavy-duty vehicles entering the urban areas of Beijing may

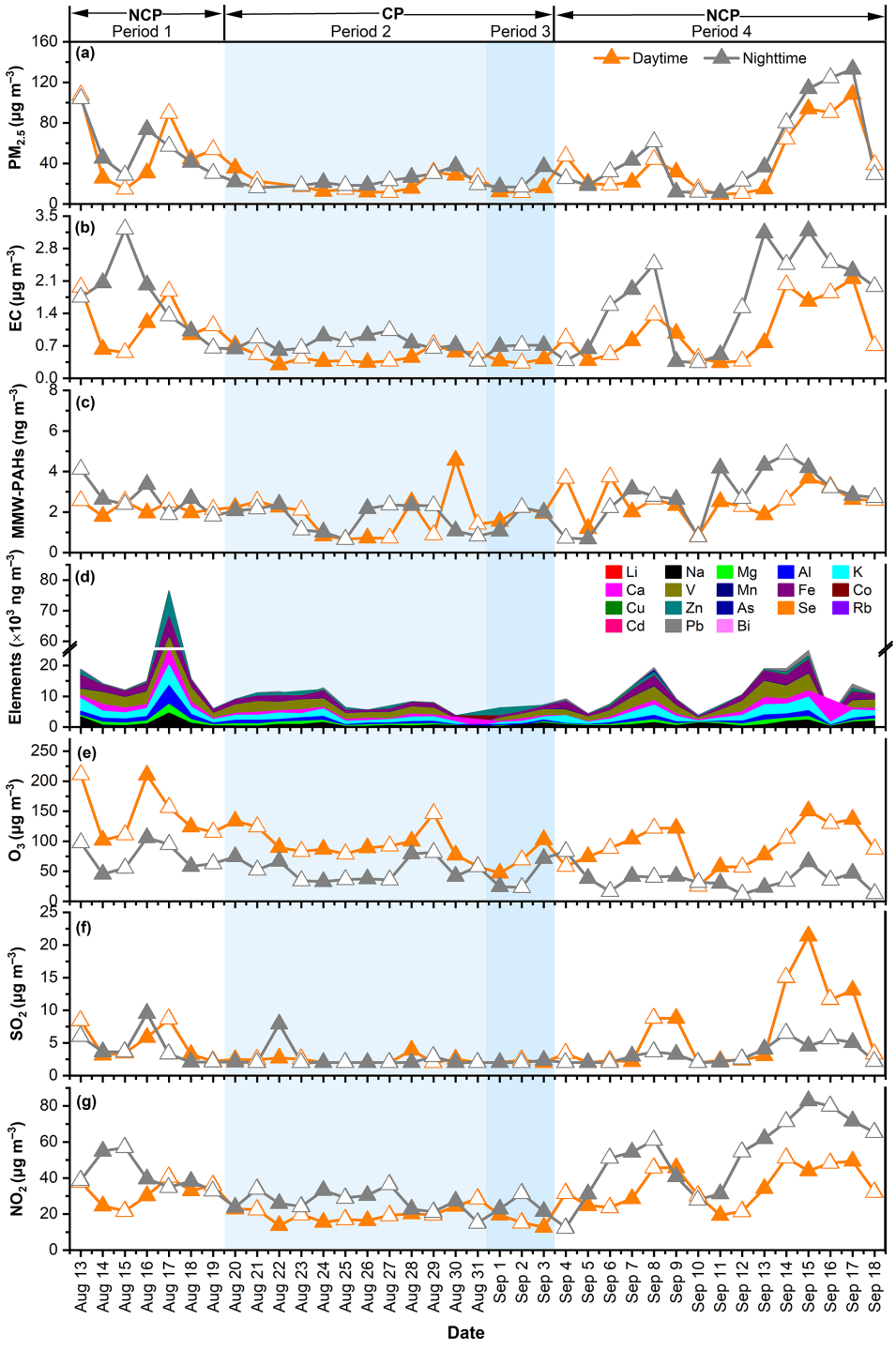

Figure 1. Temporal variations in concentrations of **(a)** $PM_{2.5}$, **(b)** EC, **(c)** MMW-PAHs, **(d)** elements, **(e)** O_3, **(f)** SO_2, and **(g)** NO_2 during the four sub-periods of the 2015 China Victory Day Parade.

lead to increased emissions from diesel vehicles near the fourth- and fifth-ring roads at night as these vehicles are allowed to enter only at night (Cai et al., 2020). Similar diurnal variations have also been observed previously in Beijing and Agra (Pipal et al., 2014; Lin et al., 2009; Ke et al., 2017; Cai et al., 2020). Additionally, lower temperatures and reduced solar radiation at night decrease the photolysis of NO_2 (Cai and Xie, 2010), further contributing to the elevated NO_2 concentrations at night. O_3 was higher in the daytime than in the nighttime, indicating intensive photochemical actions. SO_2

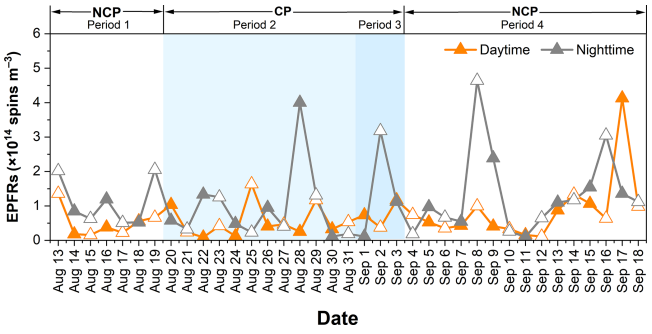

Figure 2. Temporal variations in EPFR concentrations during the measurement period.

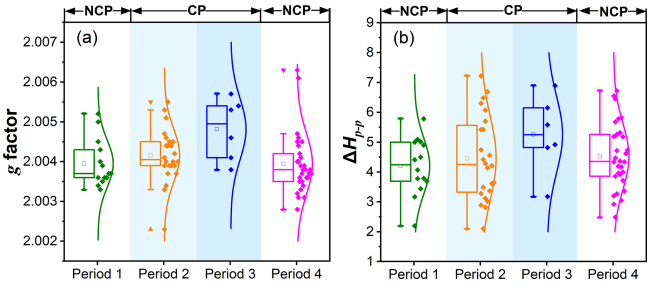

Figure 3. The **(a)** g factor and **(b)** ΔH_{p-p} of EPFRs during the four pollution periods.

concentration significantly increased in the daytime during period 4, which may be caused by the surge in industrial activities (He et al., 2017).

3.2 Characteristics of environmentally persistent free radicals (EPFRs)

Figure 2 shows the temporal variations in EPFR concentrations during the whole measurement period. The average concentration of EPFRs was $(1.00 \pm 0.75) \times 10^{14}$ spins m^{-3} during the NCP and $(8.19 \pm 5.60) \times 10^{13}$ spins m^{-3} during the CP, which represents an 18.3 % lower concentration during the CP than during the NCP. The percentage decrease in EPFRs was smaller than that in most of the other measured pollutants ($PM_{2.5}$, EC, elements, NO_2, and SO_2). Notably, despite the reduction in $PM_{2.5}$ concentration during period 3, the concentration of EPFRs paradoxically increased. Chen et al. (2020) showed that the variations in EPFR concentrations are unrelated to the variations in PM concentration and are rather determined by their source characteristics. These results suggest that variations in source contributions during the parade, such as increased contributions from traffic and other sources, may influence the formation of EPFRs. A detailed discussion of these source characteristics is provided in the subsequent source apportionment section. Furthermore, the levels of EPFRs in $PM_{2.5}$ in this study were approximately 2 orders of magnitude lower than those in Beijing (1.70×10^{15}–3.50×10^{16} spins m^{-3}) in 2016 (Yang et al., 2017) and were slightly lower than those in Xi'an (1.79×10^{14} spins m^{-3}) in 2017 (Y. Wang et al., 2019), but they were much higher than those in Chongqing (7.0×10^{13} spins m^{-3}) in 2017–2018 (Qian et al., 2020).

The average concentration of EPFRs during the daytime and nighttime were 6.85×10^{13} and 1.18×10^{14} spins m^{-3}, respectively, indicating that the nighttime samples contained more EPFRs than the daylight samples. The lower EPFR concentration during the daytime may be related to the rapid conversion of EPFRs to other chemical species under strong irradiation (Jia et al., 2019). For instance, semiquinone radicals can rapidly degrade into CO_2 under light irradiation conditions (Li et al., 2014). Previous studies have shown that the half-life times of EPFRs are shorter under light conditions than under dark conditions (Lang et al., 2022; Chen et al., 2019a), suggesting that light irradiation promotes the transformation of EPFRs. In addition, increased traffic emissions during the nighttime, as mentioned above, may have led to higher levels of EPFRs during the nighttime. For instance, Hwang et al. (2021) found that $PM_{2.5}$ from traffic-related sources generally has higher EPFR concentrations than that from urban background particles.

The g factor and ΔH_{p-p} values of EPFRs during the four pollution periods are depicted in Fig. 3. The average g factor was 2.00395 in the NCP and 2.00429 in the CP. Hence, the observed EPFRs in the NCP tend to be radical-centered on a mixture of carbon and oxygen. The higher g factor in the CP, especially in period 3, suggested that oxygen-centered free radicals were attached to the $PM_{2.5}$ samples (Li et al., 2023). It has been reported in the literature that EPFRs derived from primary-combustion sources (e.g., coal combustion and vehicle emissions) generally have a lower g factor (Chen et al., 2019c). The data presented above indicated that the generation of EPFRs with lower g factor decreased during the CP when the emissions from combustion sources were significantly reduced. It is known that carbon-centered radicals are more unstable and easily oxidized in the atmosphere than oxygen-centered radicals (Wang et al., 2018). Therefore, the free radicals generated during the CP were less susceptible to further oxidation, while those generated during the NCP were more easily oxidized. The average ΔH_{p-p} of EPFRs during the NCP and the CP was 4.42 ± 0.87 and 4.62 ± 1.06 G, respectively. The slightly larger ΔH_{p-p} during the CP compared to during the NCP indicates a relatively complex path for the formation of EPFRs under strict control measures. This may be explained by a marked increase in the activity of other sources, which will be discussed below. However, current evidence is insufficient to fully explain the variations in EPFRs, and further investigations are needed to elucidate the underlying mechanisms involved.

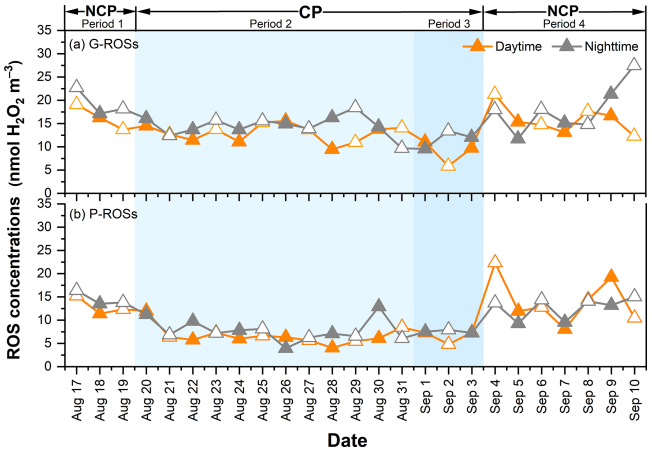

Figure 4. The concentrations of **(a)** G-ROSs and **(b)** P-ROSs during the whole measurement period.

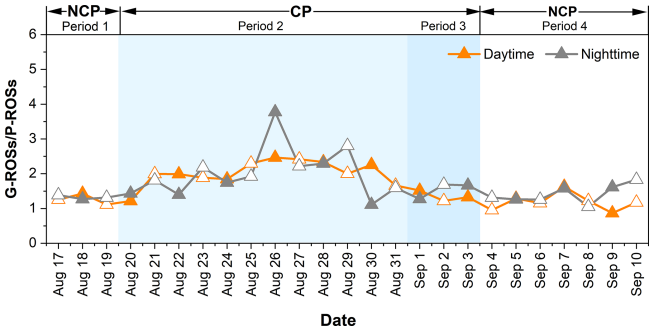

Figure 5. The ratios of G-ROSs to P-ROSs during the whole measurement period.

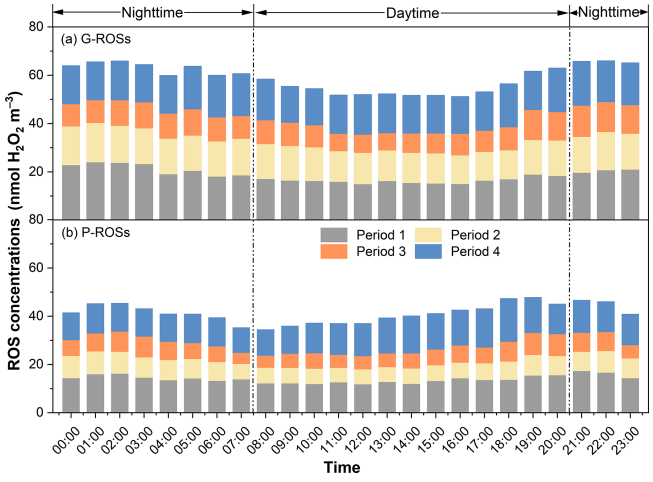

Figure 6. Diurnal variations in the concentrations of **(a)** G-ROSs and **(b)** P-ROSs during the four pollution periods.

3.3 Characteristics of reactive oxygen species (ROS) activity

The ROS activity obtained here was expressed in nmol H_2O_2 equivalents m^{-3}. As shown in Fig. 4, the average concentrations of G-ROSs and P-ROSs were 17.2 ± 2.51 and 13.6 ± 2.71 nmol H_2O_2 m^{-3}, respectively, during the NCP; decreased to 13.8 ± 1.29 and 7.25 ± 1.79 nmol H_2O_2 m^{-3} during period 2; and further decreased to 10.3 ± 0.63 and 7.02 ± 0.57 nmol H_2O_2 m^{-3} during period 3. The concentrations of ROSs during the CP were comparable to those observed in rural China (Zhao et al., 2023; Huang et al., 2016) and urban America (Wang et al., 2011). Notably, the impacts of the control measures on G-ROSs and P-ROSs were different. Compared with that of the NCP, the percentage decrease in G-ROSs during the CP was 24.1 %, which was lower than the decrease in P-ROSs of 46.9 %. This difference may be related to the complex formation and transformation mechanism of G-ROSs. These results further suggest that the percentage decreases in gaseous pollutants were smaller than those in particulate pollutants. Furthermore, the much higher ratios of G-ROSs to P-ROSs during the CP than during the NCP suggested that the contribution of G-ROSs to the atmospheric oxidizing capacity was increased or that of P-ROSs was decreased during this period (Fig. 5).

The average concentration of G-ROSs was higher during the nighttime (15.8 nmol H_2O_2 m^{-3}) than during the daytime (13.7 nmol H_2O_2 m^{-3}); this was also the was the case for P-ROSs (10.0 nmol H_2O_2 m^{-3} versus 9.5 nmol H_2O_2 m^{-3}), consistently with what was reported in a previous study conducted in Xi'an in 2021 (Ainur et al., 2023). The higher ROS levels at night are more evident from the diurnal variations shown in Fig. 6. G-ROSs decreased at approximately 08:00 LT and then rapidly increased at 17:00 LT during all four of the sub-periods. However, P-ROSs decreased at approximately 03:00 LT and then increased at approximately 13:00 LT. These results suggest that different formation mechanisms existed between G-ROSs and P-ROSs.

3.4 Correlation analysis

Figure 7 shows the Spearman correlation of EPFRs, G-ROSs, and P-ROSs with other pollutants. The EPFR concentrations are strongly correlated with ΔH_{p-p} ($r > 0.76$), indicating more abundant types of EPFRs under higher EPFR concentrations. In addition to simple and well-defined EPFRs, such as semiquinone and cyclopentadienyl radicals, there are also many complex and unknown EPFRs in the research blind spots. Air quality index (AQI) and $PM_{2.5}$ were both positively correlated with the concentration of EPFRs ($r > 0.42$), suggesting that the contamination of EPFRs was significantly influenced by the relevant health index and haze. EPFRs exhibited a significant positive correlation with the vehicle exhaust markers EC and NO_2 ($p < 0.05$), emphasizing that vehicle exhaust emissions may be an important source of EPFRs in Beijing. Recent studies also found that EPFRs were significantly correlated with EC and NO_2 on high-

ways, mainly attributed to the emissions from vehicle exhausts (Hwang et al., 2021; Li et al., 2022). A stronger positive correlation between EPFRs and secondary inorganic ions was found in the daytime ($r = 0.45$) than during the nighttime ($r = 0.37$). Meanwhile, a significant positive correlation between EPFRs and O_3 was also observed in the daytime ($p < 0.1$), consistently with the results of Chen et al. (2019b). The oxidation of different types of PAHs by O_3 could form different types of EPFRs, as demonstrated in a previous study (Borrowman et al., 2016). However, Hwang et al. (2021) observed a negative correlation between EPFRs and O_3 at highway sites, attributed to the consumption of O_3 by NO. In this study, hot summer conditions may be conducive to the conversion of PAHs into EPFRs, especially in environments with relatively high O_3 concentrations. This implies that the mechanism of EPFR generation varies under different environmental conditions. Transition metals, such as single-electron acceptors or shuttles (Wan et al., 2020), play a key role not only in the formation of EPFRs but also in maintaining the long half-life of EPFRs (Pan et al., 2019; Vinayak et al., 2022). Cd was significantly correlated with EPFRs only during the daytime ($p < 0.05$), while the majority of transition metals (e.g., Mn, Fe, V, and Cd) were significantly correlated with EPFRs during the nighttime. These results suggest that EPFRs at night are stabilized in particles via transition metals from fuel combustion processes, while an increased proportion of EPFRs were generated via other pathways in the daytime, such as the secondary reactions mentioned above.

It is not surprising that P-ROSs were associated with $PM_{2.5}$ more than G-ROSs were. Both G-ROSs and P-ROSs were strongly correlated with EC and NO_2 ($r > 0.54$) during the daytime, suggesting that G-ROSs and P-ROSs were derived from traffic-related emissions, as was reported in a previous study (Stevanovic et al., 2019). G-ROSs ($r > 0.52$) and P-ROSs ($r > 0.54$) were also well correlated with secondary inorganic ions in the daytime, indicating secondary aerosols as another important source of G-ROSs and P-ROSs. G-ROSs were significantly correlated with the majority of transition metals (e.g., V, Mn, Fe, Co, Cu, and Cd) ($p < 0.1$), and P-ROSs were positively correlated with metals (e.g., V, Mn, Co, and Cd), which is consistent with the current knowledge regarding the metal-induced ROS formation mechanism. Transition metals have been considered to be capable of generating excess ROSs such as $OH^{\bullet}$ and $^{\bullet}O_2^-$ via Fenton-like reactions (Brehmer et al., 2019; Lin and Yu, 2020).

During the nighttime, there were moderate correlations between P-ROSs and AQI, NO_2, SO_2, and secondary inorganic ions, indicating the contributions of vehicle exhaust emissions and coal combustion emissions, as well as the secondary formation to P-ROSs. The very weak correlation of both G-ROSs and P-ROSs with O_3 implied the limited formation of G-ROSs and P-ROSs from secondary reaction processes caused by O_3 in Beijing. The correlations of G-ROSs and P-ROSs with EPFRs were also very weak. Although EPFRs can induce the formation of single ROS species (e.g., $OH^{\bullet}$ and $^{\bullet}O_2^-$) (Hwang et al., 2021; Guo et al., 2020), individual ROS species cannot exist alone in the air, leading to different interactions between EPFRs and different ROS species.

3.5 Source apportionment

The source profiles of $PM_{2.5}$ were analyzed using the PMF model. As shown in Fig. 8, when considering the whole campaign together, five major source factors were identified. The high proportions of NO_3^-, SO_4^{2-}, and NH_4^+ are attributed to secondary aerosols. One factor is recognized as vehicle emissions due to the high abundance of EC and Cu. Another factor is related to dust sources because of the high proportions of Mg, Al, Ca, and Fe. A fourth factor is linked to industrial emission sources due to the high proportions of V, Mn, Rb, Cd, Pb, and Bi. Additionally, a fifth factor is identified as "other sources" because of the high abundance of Co and Zn. Secondary aerosols accounted for the largest fraction (52.0 %), followed by vehicle emissions (20.8 %), dust sources (13.5 %), other sources (7.4 %), and industrial emissions (6.3 %), the total of which resolved 95.4 % of the total $PM_{2.5}$. The percentage contributions from each source factor to $PM_{2.5}$ differed to some extent between the NCP and the CP (Fig. 9). For example, the percentage contributions from the above five source factors were 55.0 %, 17.5 %, 15.6 %, 5.22 %, and 6.70 %, respectively, during the NCP (Fig. S1) and were 30.5 %, 30.8 %, 15.1 %, 17.9 %, and 5.77 %, respectively, during the CP. The large decrease in the percentage contribution from secondary aerosols during the CP was due to the tremendous reductions in precursor gases (e.g., SO_2 and NO_2) of secondary aerosols. The percentage contribution from vehicle emissions actually increased because the concentration decrease from this sector was smaller than that from the other major source sectors (especially the factor of secondary aerosols). During period 2, the World Athletics Championships held at the National Stadium (known as the Bird's Nest) likely resulted in increased traffic flow around the sampling site, thus moderating the decrease in concentrations from vehicle emissions during the CP.

The concentrations of $PM_{2.5}$ fractions from most source factors decreased during the CP compared to the NCP (Fig. S2), e.g., by 78.7 %, 32.6 %, 63.0 %, and 67.0 % from secondary aerosols, vehicle emissions, dust sources, and industrial emissions, respectively, due to the strict emission control measures implemented during the CP. Thus, the achievement of Parade Blue days was largely attributed to dramatic decreases in secondary aerosols, dust sources, and industrial emissions, a phenomenon that is consistent with that observed in a previous study during the Asia-Pacific Economic Cooperation conference conducted by Sun et al. (2016). Obviously, the strict control measures during the parade period effectively reduced both primary and secondary pollutants.

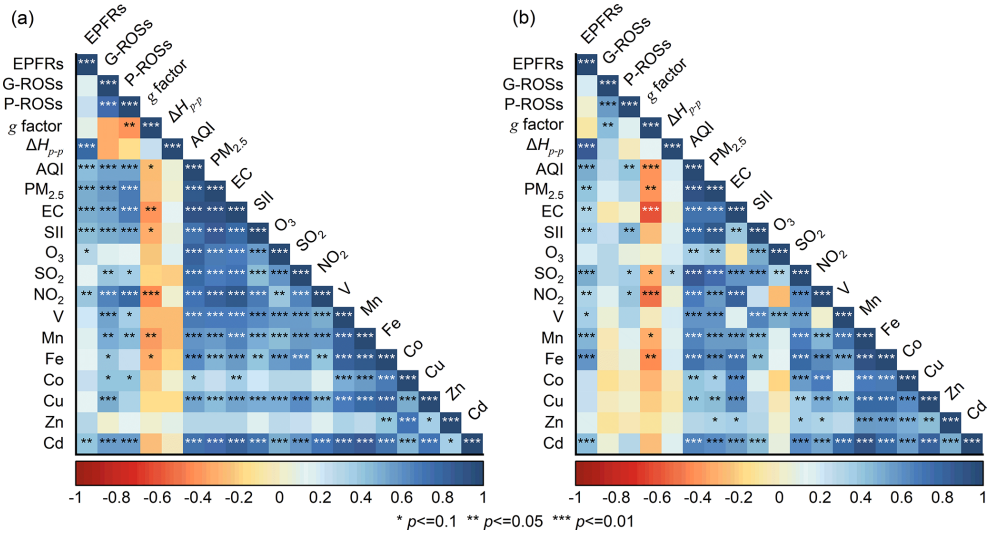

Figure 7. Spearman correlation matrix of EPFR, G-ROS, and P-ROS concentrations, with meteorological parameters, gaseous pollutants, and $PM_{2.5}$ components during **(a)** daytime and **(b)** nighttime. SII: secondary inorganic ions. Red and blue colors denote a negative and a positive correlation, respectively.

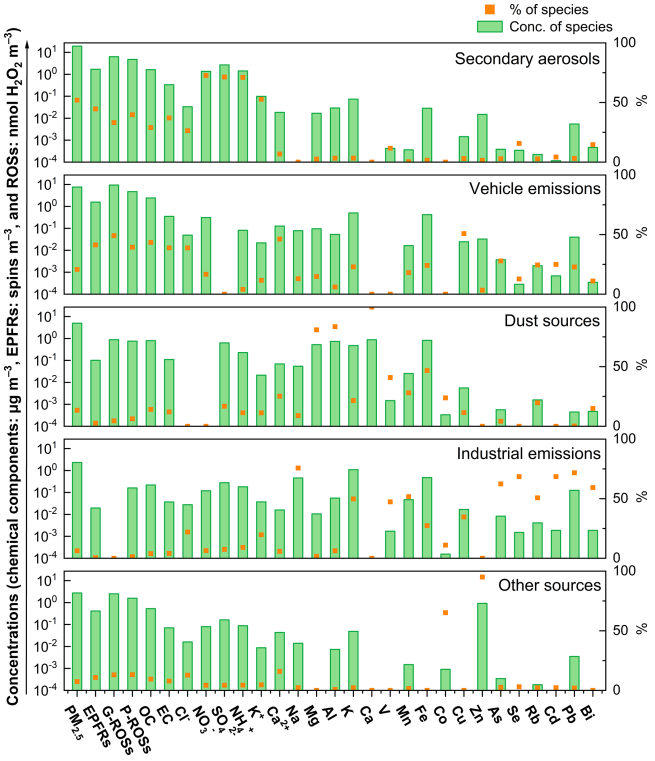

Figure 8. Profiles of different source factors of $PM_{2.5}$.

The predominant sources of EPFRs during the NCP were also secondary aerosols (50.6 %), followed by vehicle emissions (33.5 %), other sources (9.89 %), dust sources (4.12 %), and industrial emissions (1.85 %). The percentage contributions of these source sectors to EPFRs during the CP changed to 20.8 %, 43.7 %, 31.2 %, 3.01 %, and 1.27 %, respectively. Vehicle emissions surpassed secondary aerosols to become the largest source of EPFRs during the CP. Additionally, contributions from other sources also significantly increased during the CP, especially during period 3. During the NCP, secondary aerosols were also the largest source (45.9 %) of G-ROSs, followed by vehicle emissions (36.6 %), dust sources (11.2 %), other sources (5.78 %), and industrial emissions (0.54 %). During the CP, the contribution of secondary aerosols decreased remarkably to 18.3 %, while that of vehicle emissions increased significantly to 43.0 %, and that of other sources increased significantly to 29.5 %. Similarly, the predominant source of P-ROSs during the NCP was also secondary aerosols (44.3 %), followed by vehicle emissions (30.0 %), dust sources (12.9 %), other sources (10.0 %), and industrial emissions (2.73 %). During the CP, the contribution of secondary aerosols (17.7 %) to P-ROSs dropped significantly, while that of vehicle emissions and other sources increased significantly to 35.2 % and 35.8 %, respectively. Although most pollutants were effectively regulated during the CP, the levels of hazardous substances such as EPFRs and ROSs failed to decrease simultaneously. The PMF results imply that the role of inadequately controlled vehicle emissions and other sources in air quality and public health may be more complex than expected.

4 Conclusions

The short-term air quality control measures on hazardous substances during the 2015 China Victory Day Parade in Beijing reduced the concentrations of EPFRs by 18.3 % and those of G-ROSs and P-ROSs by 24.1 % and 46.9 %, respec-

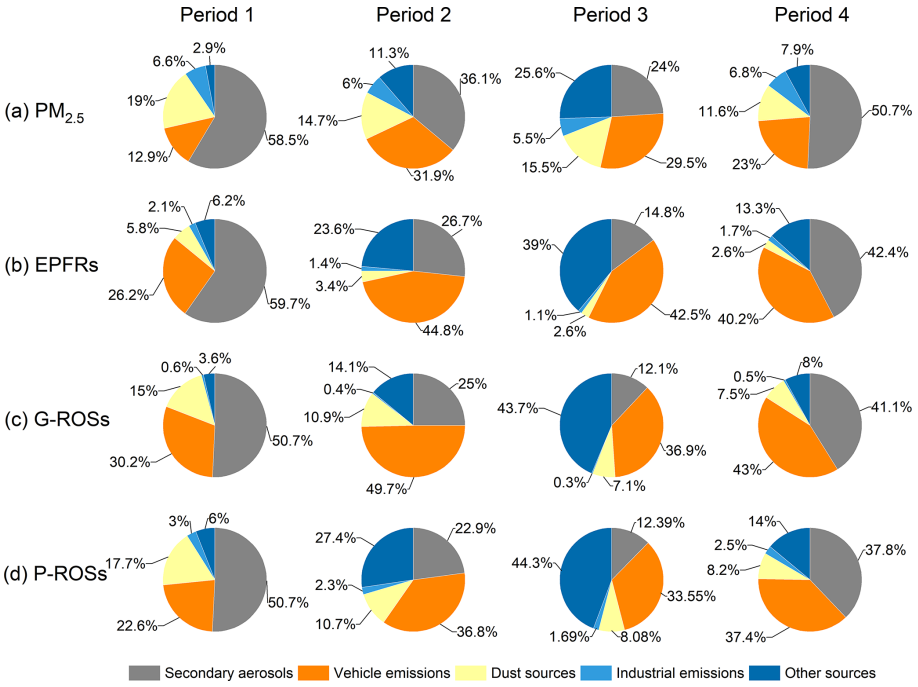

Figure 9. The contributions of different sources to **(a)** $PM_{2.5}$, **(b)** EPFRs, **(c)** G-ROSs, and **(d)** P-ROSs during the four sub-period.

tively, during the CP compared to during the NCP. Overall, the decreases in EPFRs and ROSs were smaller than those for most other measured pollutants (e.g., $PM_{2.5}$, EC, elements, and SO_2). Although particle-matter-based air quality control measures have performed well in achieving Parade Blue, it is difficult to simultaneously reduce the negative impacts of the atmosphere on human health. Given that EPFRs and ROSs exhibited a significant positive correlation ($p < 0.01$) with EC, secondary inorganic ions, NO_2, and Cd, controlling the emissions of these chemical species would reduce EPFR and ROS pollution. The sources of EPFRs and ROSs differed between daytime and nighttime. EPFRs were mainly from vehicle exhaust emissions and atmospheric oxidation processes in the daytime and from vehicle exhaust emissions and fossil fuel combustion in the nighttime. Vehicle exhausts, secondary aerosols, and metals from fuel combustion processes were important sources of G-ROSs and P-ROSs in the daytime, while vehicle exhaust and coal combustion emissions were the major contributors of P-ROSs in the nighttime. The predominant sources of $PM_{2.5}$, EPFRs, G-ROSs, and P-ROSs during the NCP were secondary aerosols, followed by vehicle emissions, but vehicle emissions surpassed secondary aerosols to become the predominant source of these chemical species during the CP. The control measures implemented during the CP reduced source-sector-based concentrations of $PM_{2.5}$, EPFRs, G-ROSs, and P-ROSs by 78.7 %–80.8 % when coming from secondary aerosols, by 59.3 %–65.0 % when coming from dust sources, by 65.3 %–67.0 % when coming from industrial emissions, and by 32.6 %–43.8 % when coming from vehicle emissions, while concentrations from other sources increased by 1.61 %–71.5 % compared to the cases during the NCP. Results from this study will benefit the development of future air quality management policies targeting EPFRs and ROSs. However, the generation and transformation processes of EPFRs and ROSs involve multiple complex chemical reactions, and further in-depth studies are still needed to gain a complete understanding of the formation pathways of EPFRs and ROSs under different environmental conditions. For example, it is necessary to conduct smog chamber or flow tube experiments to simulate the photochemical reactions and oxidation processes of EPFRs and ROSs in the atmosphere. In addition, further development and optimization of pretreatment and analytical techniques are needed to isolate different types of EPFRs and to obtain detailed information such as g-tensor and hyperfine-splitting constants. This is crucial for revealing the specific structures of radicals and thereby clarifying the relationship between EPFRs and ROSs.

Data availability. The data used in this study are available on the Zenodo data repository platform: https://doi.org/10.5281/zenodo.10136894 (Qin et al., 2023).

Supplement. The supplement related to this article is available online at: https://doi.org/10.5194/acp-24-8737-2024-supplement.

Author contributions. YZ and JT: conceptualization and writing – review and editing. YQ: writing – original draft and writing – review and editing. XZ: writing – review and editing. WH: investigation. JQ: methodology. XH: software. YC: investigation. TZ: software. ZZ: investigation. XW: methodology. ZW: funding acquisition.

Competing interests. The contact author has declared that none of the authors has any competing interests.

Disclaimer. Publisher's note: Copernicus Publications remains neutral with regard to jurisdictional claims made in the text, published maps, institutional affiliations, or any other geographical representation in this paper. While Copernicus Publications makes every effort to include appropriate place names, the final responsibility lies with the authors.

Acknowledgements. The authors thank the editor and anonymous reviewers for their valuable suggestions.

Financial support. This research has been supported by the National Key Research and Development Program of China (grant nos. 2022YFC3703000, 2023YFE0102400, 2022YFC3703402, and 2022YFC3701103) and the Provincial Natural Science Foundation of Hunan (grant no. 2023JJ30004).

Review statement. This paper was edited by Steven Brown and reviewed by two anonymous referees.

References

Ainur, D., Chen, Q., Sha, T., Zarak, M., Dong, Z., Guo, W., Zhang, Z., Dina, K., and An, T.: Outdoor health risk of atmospheric particulate matter at night in Xi'an, northwestern China, Environ. Sci. Technol., 57, 9252–9265, https://doi.org/10.1021/acs.est.3c02670, 2023.

Arangio, A. M., Tong, H., Socorro, J., Pöschl, U., and Shiraiwa, M.: Quantification of environmentally persistent free radicals and reactive oxygen species in atmospheric aerosol particles, Atmos. Chem. Phys., 16, 13105–13119, https://doi.org/10.5194/acp-16-13105-2016, 2016.

Bates, J. T., Fang, T., Verma, V., Zeng, L., Weber, R. J., Tolbert, P. E., Abrams, J. Y., Sarnat, S. E., Klein, M., and Mulholland, J. A.: Review of acellular assays of ambient particulate matter oxidative potential: methods and relationships with composition, sources, and health effects, Environ. Sci. Technol., 53, 4003–4019, https://doi.org/10.1021/acs.est.8b03430, 2019.

Borrowman, C. K., Zhou, S., Burrow, T. E., and Abbatt, J. P.: Formation of environmentally persistent free radicals from the heterogeneous reaction of ozone and polycyclic aromatic compounds, Phys. Chem. Chem. Phys., 18, 205–212, https://doi.org/10.1039/C5CP05606C, 2016.

Brehmer, C., Lai, A., Clark, S., Shan, M., Ni, K., Ezzati, M., Yang, X., Baumgartner, J., Schauer, J. J., and Carter, E.: The oxidative potential of personal and household $PM_{2.5}$ in a rural setting in southwestern China, Environ. Sci. Technol., 53, 2788–2798, https://doi.org/10.1021/acs.est.8b05120, 2019.

Cai, H. and Xie, S. D.: A modelling study of air quality impact of odd-even day traffic restriction scheme before, during and after the 2008 Beijing Olympic Games, Atmos. Chem. Phys. Discuss., 10, 5135–5184, https://doi.org/10.5194/acpd-10-5135-2010, 2010.

Cai, J., Chu, B., Yao, L., Yan, C., Heikkinen, L. M., Zheng, F., Li, C., Fan, X., Zhang, S., Yang, D., Wang, Y., Kokkonen, T. V., Chan, T., Zhou, Y., Dada, L., Liu, Y., He, H., Paasonen, P., Kujansuu, J. T., Petäjä, T., Mohr, C., Kangasluoma, J., Bianchi, F., Sun, Y., Croteau, P. L., Worsnop, D. R., Kerminen, V.-M., Du, W., Kulmala, M., and Daellenbach, K. R.: Size-segregated particle number and mass concentrations from different emission sources in urban Beijing, Atmos. Chem. Phys., 20, 12721–12740, https://doi.org/10.5194/acp-20-12721-2020, 2020.

Chen, Q., Wang, M., Sun, H., Wang, X., Wang, Y., Li, Y., Zhang, L., and Mu, Z.: Enhanced health risks from exposure to environmentally persistent free radicals and the oxidative stress of $PM_{2.5}$ from Asian dust storms in Erenhot, Zhangbei and Jinan, China, Environ. Int., 121, 260–268, https://doi.org/10.1016/j.envint.2018.09.012, 2018a.

Chen, Q., Sun, H., Wang, M., Mu, Z., Wang, Y., Li, Y., Wang, Y., Zhang, L., and Zhang, Z.: Dominant fraction of EPFRs from nonsolvent-extractable organic matter in fine particulates over Xi'an, China, Environ. Sci. Technol., 52, 9646–9655, https://doi.org/10.1021/acs.est.8b01980, 2018b.

Chen, Q., Sun, H., Wang, M., Wang, Y., Zhang, L., and Han, Y.: Environmentally persistent free radical (EPFR) formation by visible-light illumination of the organic matter in atmospheric particles, Environ. Sci. Technol., 53, 10053–10061, https://doi.org/10.1021/acs.est.9b02327, 2019a.

Chen, Q., Sun, H., Mu, Z., Wang, Y., Li, Y., Zhang, L., Wang, M., and Zhang, Z.: Characteristics of environmentally persistent free radicals in $PM_{2.5}$: Concentrations, species and sources in Xi'an, Northwestern China, Environ. Pollut., 247, 18–26, https://doi.org/10.1016/j.envpol.2019.01.015, 2019b.

Chen, Q., Sun, H., Wang, J., Shan, M., Yang, X., Deng, M., Wang, Y., and Zhang, L.: Long-life type – The dominant fraction of EPFRs in combustion sources and ambient fine particles in Xi'an, Atmos. Environ., 219, 117059, https://doi.org/10.1016/j.atmosenv.2019.117059, 2019c.

Chen, Q., Sun, H., Song, W., Cao, F., Tian, C., and Zhang, Y.-L.: Size-resolved exposure risk of persistent free radicals (PFRs) in atmospheric aerosols and their potential sources, Atmos. Chem. Phys., 20, 14407–14417, https://doi.org/10.5194/acp-20-14407-2020, 2020.

Dellinger, B., Pryor, W. A., Cueto, R., Squadrito, G. L., Hegde, V., and Deutsch, W. A.: Role of free radicals in the toxicity of airborne fine particulate matter, Chem. Res. Toxicol., 14, 1371–1377, https://doi.org/10.1021/tx010050x, 2001.

Dugas, T. R., Lomnicki, S., Cormier, S. A., Dellinger, B., and Reams, M.: Addressing emerging risks: Scientific and regulatory challenges associated with environmentally persistent free radicals, Int. J. Env. Res. Pub. He., 13, 573, https://doi.org/10.3390/ijerph13060573, 2016.

Fang, T., Guo, H., Zeng, L., Verma, V., Nenes, A., and Weber, R. J.: Highly acidic ambient particles, soluble metals, and oxidative potential: A link between sulfate and aerosol toxicity, Environ. Sci. Technol., 51, 2611–2620, https://doi.org/10.1021/acs.est.6b06151, 2017.

Fang, T., Hwang, B. C., Kapur, S., Hopstock, K. S., Wei, J., Nguyen, V., Nizkorodov, S. A., and Shiraiwa, M.: Wildfire particulate matter as a source of environmentally persistent free radicals and reactive oxygen species, Environmental Science: Atmospheres, 3, 581–594, https://doi.org/10.1039/D2EA00170E, 2023.

Gehling, W., Khachatryan, L., and Dellinger, B.: Hydroxyl radical generation from environmentally persistent free radicals (EPFRs) in $PM_{2.5}$, Environ. Sci. Technol., 48, 4266–4272, https://doi.org/10.1021/es401770y, 2014.

Guo, J., He, J., Liu, H., Miao, Y., Liu, H., and Zhai, P.: Impact of various emission control schemes on air quality using WRF-Chem during APEC China 2014, Atmos. Environ., 140, 311–319, https://doi.org/10.1016/j.atmosenv.2016.05.046, 2016.

Guo, X., Zhang, N., Hu, X., Huang, Y., Ding, Z., Chen, Y., and Lian, H.: Characteristics and potential inhalation exposure risks of $PM_{2.5}$–bound environmental persistent free radicals in Nanjing, a mega–city in China, Atmos. Environ., 224, 117355, https://doi.org/10.1016/j.atmosenv.2020.117355, 2020.

He, Z., Shi, X., Wang, X., and Xu, Y.: Urbanisation and the geographic concentration of industrial SO_2 emissions in China, Urban. Stud., 54, 3579–3596, https://doi.org/10.1177/0042098016669915, 2017.

Hien, P., Hangartner, M., Fabian, S., and Tan, P.: Concentrations of NO_2, SO_2, and benzene across Hanoi measured by passive diffusion samplers, Atmos. Environ., 88, 66–73, https://doi.org/10.1016/j.atmosenv.2014.01.036, 2014.

Hu, Y., Zhang, B., Guo, Q., Wang, S., and Lu, S.: Characterization into environmentally persistent free radicals formed in incineration fly ash and pyrolysis biochar of sewage sludge and biomass, J. Clean. Prod., 373, 133666, https://doi.org/10.1016/j.jclepro.2022.133666, 2022.

Huang, J., Pan, X., Guo, X., and Li, G.: Health impact of China's air pollution prevention and control action plan: An analysis of national air quality monitoring and mortality data, Lancet Planet. Health., 2, e313–e323, https://doi.org/10.1016/S2542-5196(18)30141-4, 2018.

Huang, W., Zhang, Y., Zhang, Y., Zeng, L., Dong, H., Huo, P., Fang, D., and Schauer, J. J.: Development of an automated sampling-analysis system for simultaneous measurement of reactive oxygen species (ROS) in gas and particle phases: GAC-ROS, Atmos. Environ., 134, 18–26, https://doi.org/10.1016/j.atmosenv.2016.03.038, 2016.

Huang, W., Fang, D., Shang, J., Li, Z., Zhang, Y., Huo, P., Liu, Z., Schauer, J. J., and Zhang, Y.: Relative impact of short-term emissions controls on gas and particle-phase oxidative potential during the 2015 China Victory Day Parade in Beijing, China, Atmos. Environ., 183, 49–56, https://doi.org/10.1016/j.atmosenv.2018.03.046, 2018.

Hwang, B., Fang, T., Pham, R., Wei, J., Gronstal, S., Lopez, B., Frederickson, C., Galeazzo, T., Wang, X., and Jung, H.: Environmentally persistent free radicals, reactive oxygen species generation, and oxidative potential of highway $PM_{2.5}$, ACS Earth Space. Chem., 5, 1865–1875, https://doi.org/10.1021/acsearthspacechem.1c00135, 2021.

Jia, H., Zhao, S., Shi, Y., Zhu, K., Gao, P., and Zhu, L.: Mechanisms for light-driven evolution of environmentally persistent free radicals and photolytic degradation of PAHs on Fe(III)-montmorillonite surface, J. Hazard. Mater., 362, 92–98, https://doi.org/10.1016/j.jhazmat.2018.09.019, 2019.

Ke, W., Zhang, S., Wu, Y., Zhao, B., Wang, S., and Hao, J.: Assessing the future vehicle fleet electrification: The impacts on regional and urban air quality, Environ. Sci. Technol., 51, 1007–1016, https://doi.org/10.1021/acs.est.6b04253, 2017.

Khan, F., Garg, V. K., Singh, A. K., and Kumar, T.: Role of free radicals and certain antioxidants in the management of huntington's disease: A review, J. Anal. Pharm. Res, 7, 386–392, https://doi.org/10.15406/japlr.2018.07.00256, 2018.

Lang, D., Jiang, F., Gao, X., Yi, P., Liu, Y., Li, H., Chen, Q., Pan, B., and Xing, B.: Generation of environmentally persistent free radicals on faceted TiO_2 in an ambient environment: roles of crystalline surface structures, Environ. Sci. Nano., 9, 2521–2533, https://doi.org/10.1039/D2EN00240J, 2022.

Li, H., Pan, B., Liao, S., Zhang, D., and Xing, B.: Formation of environmentally persistent free radicals as the mechanism for reduced catechol degradation on hematite-silica surface under UV irradiation, Environ. Pollut., 188, 153–158, https://doi.org/10.1016/j.envpol.2014.02.012, 2014.

Li, H., Chen, Q., Wang, C., Wang, R., Sha, T., Yang, X., and Ainur, D.: Pollution characteristics of environmental persistent free radicals (EPFRs) and their contribution to oxidation potential in road dust in a large city in northwest China, J. Hazard. Mater., 442, 130087, https://doi.org/10.1016/j.jhazmat.2022.130087, 2023.

Li, Z., Zhao, H., Li, X., and Bekele, T. G.: Characteristics and sources of environmentally persistent free radicals in $PM_{2.5}$ in Dalian, Northeast China: correlation with polycyclic aromatic hydrocarbons, Environ. Sci. Pollut. Res., 29, 24612–24622, https://doi.org/10.1007/s11356-021-17688-9, 2022.

Lin, M. and Yu, J. Z.: Assessment of interactions between transition metals and atmospheric organics: Ascorbic acid depletion and hydroxyl radical formation in organic-metal mixtures, Environ. Sci. Technol., 54, 1431–1442, https://doi.org/10.1021/acs.est.9b07478, 2020.

Lin, P., Hu, M., Deng, Z., Slanina, J., Han, S., Kondo, Y., Takegawa, N., Miyazaki, Y., Zhao, Y., and Sugimoto, N.: Seasonal and diurnal variations of organic carbon in $PM_{2.5}$ in Beijing and the estimation of secondary organic carbon, J. Geophys. Res., 114, D00G11, https://doi.org/10.1029/2008JD010902, 2009.

Ma, X., Li, C., Dong, X., and Liao, H.: Empirical analysis on the effectiveness of air quality control measures during mega events: evidence from Beijing, China, J. Clean. Prod., 271, 122536, https://doi.org/10.1016/j.jclepro.2020.122536, 2020.

Niu, Y., Li, X., Qi, B., and Du, R.: Variation in the concentrations of atmospheric $PM_{2.5}$ and its main chemical components in an eastern China city (Hangzhou) since the release of the Air Pollution Prevention and Control Action Plan in 2013, Air Qual. Atmos. Health., 15, 321–337, https://doi.org/10.1007/s11869-021-01107-6, 2022.

Odinga, E. S., Waigi, M. G., Gudda, F. O., Wang, J., Yang, B., Hu, X., Li, S., and Gao, Y.: Occurrence, formation, environmental fate and risks of environmentally persistent free radicals in biochars, Environ. Int., 134, 105172, https://doi.org/10.1016/j.envint.2019.105172, 2020.

Okuda, T., Matsuura, S., Yamaguchi, D., Umemura, T., Hanada, E., Orihara, H., Tanaka, S., He, K., Ma, Y., Cheng, Y., and Liang, L.: The impact of the pollution control measures for the 2008 Beijing Olympic Games on the chemical composition of aerosols, Atmos. Environ., 45, 2789–2794, https://doi.org/10.1016/j.atmosenv.2011.01.053, 2011.

Pan, B., Li, H., Lang, D., and Xing, B.: Environmentally persistent free radicals: Occurrence, formation mechanisms and implications, Environ. Pollut., 248, 320–331, https://doi.org/10.1016/j.envpol.2019.02.032, 2019.

Perrone, M. G., Carbone, C., Faedo, D., Ferrero, L., Maggioni, A., Sangiorgi, G., and Bolzacchini, E.: Exhaust emissions of polycyclic aromatic hydrocarbons, n-alkanes and phenols from vehicles coming within different European classes, Atmos. Environ., 82, 391–400, https://doi.org/10.1016/j.atmosenv.2013.10.040, 2014.

Pipal, A. S., Jan, R., Bisht, D. S., Srivastava, A. K., Tiwari, S., and Taneja, A.: Day and night variability of atmospheric organic and elemental carbon during winter of 2011–12 in Agra, India, Sustain. Environ. Res., 24, 107–116, 2014.

Qian, R., Zhang, S., Peng, C., Zhang, L., Yang, F., Tian, M., Huang, R., Wang, Q., Chen, Q., Yao, X., and Chen, Y.: Characteristics and potential exposure risks of environmentally persistent free radicals in $PM_{2.5}$ in the three gorges reservoir area, Southwestern China, Chemosphere, 252, 126425, https://doi.org/10.1016/j.chemosphere.2020.126425, 2020.

Qin, Y., Zhang, X., Huang, W., Qin, J., Hu, X., Cao, Y., Zhao, T., Zhang, Y., Tan, J., Zhang, Z., Wang, X., and Wang, Z.: Measurement report: Impact of emission control measures on environmental persistent free radicals and reactive oxygen species – A short-term case study in Beijing, Zenodo [data set], https://doi.org/10.5281/zenodo.10136894, 2023.

Saravia, J., Lee, G. I., Lomnicki, S., Dellinger, B., and Cormier, S. A.: Particulate matter containing environmentally persistent free radicals and adverse infant respiratory health effects: a review, J. Biochem. Mol. Toxicol., 27, 56–68, https://doi.org/10.1002/jbt.21465, 2013.

Schleicher, N., Norra, S., Chen, Y., Chai, F., and Wang, S.: Efficiency of mitigation measures to reduce particulate air pollution – a case study during the Olympic Summer Games 2008 in Beijing, China, Sci. Total Environ., 427, 146–158, https://doi.org/10.1016/j.scitotenv.2012.04.004, 2012.

Sharma, S., Mandal, T., Jain, S., Saraswati, Sharma, A., and Saxena, M.: Source apportionment of $PM_{2.5}$ in Delhi, India using PMF model, Bull. Environ. Contam. Toxicol., 97, 286–293, https://doi.org/10.1007/s00128-016-1836-1, 2016.

Stevanovic, S., Gali, N. K., Salimi, F., Brown, R. A., Ning, Z., Cravigan, L., Brimblecombe, P., Bottle, S., and Ristovski, Z. D.: Diurnal profiles of particle-bound ROS of $PM_{2.5}$ in urban environment of Hong Kong and their association with $PM_{2.5}$, black carbon, ozone and PAHs, Atmos. Environ., 219, 117023, https://doi.org/10.1016/j.atmosenv.2019.117023, 2019.

Sun, Y., Wang, Z., Wild, O., Xu, W., Chen, C., Fu, P., Du, W., Zhou, L., Zhang, Q., Han, T., Wang, Q., Pan, X., Zheng, H., Li, J., Guo, X., Liu, J., and Worsnop, D. R.: "APEC Blue": Secondary aerosol reductions from emission controls in Beijing, Sci. Rep., 6, 20668, https://doi.org/10.1038/srep20668, 2016.

Thevenot, P. T., Saravia, J., Jin, N., Giaimo, J. D., Chustz, R. E., Mahne, S., Kelley, M. A., Hebert, V. Y., Dellinger, B., and Dugas, T. R.: Radical-containing ultrafine particulate matter initiates epithelial-to-mesenchymal transitions in airway epithelial cells, Am. J. Respir. Cell Mol. Biol., 48, 188–197, https://doi.org/10.1165/rcmb.2012-0052OC, 2013.

Tong, H., Lakey, P. S. J., Arangio, A. M., Socorro, J., Shen, F., Lucas, K., Brune, W. H., Pöschl, U., and Shiraiwa, M.: Reactive oxygen species formed by secondary organic aerosols in water and surrogate lung fluid, Environ. Sci. Technol., 52, 11642–11651, https://doi.org/10.1021/acs.est.8b03695, 2018.

Vejerano, E. P., Rao, G., Khachatryan, L., Cormier, S. A., and Lomnicki, S.: Environmentally persistent free radicals: Insights on a new class of pollutants, Environ. Sci. Technol., 52, 2468–2481, https://doi.org/10.1021/acs.est.7b04439, 2018.

Venkatachari, P., Hopke, P. K., Brune, W. H., Ren, X., Lesher, R., Mao, J., and Mitchell, M.: Characterization of wintertime reactive oxygen species concentrations in Flushing, New York, Aerosol Sci. Tech., 41, 97–111, https://doi.org/10.1080/02786820601116004, 2007.

Verma, V., Shafer, M. M., Schauer, J. J., and Sioutas, C.: Contribution of transition metals in the reactive oxygen species activity of PM emissions from retrofitted heavy-duty vehicles, Atmos. Environ., 44, 5165–5173, https://doi.org/10.1016/j.atmosenv.2010.08.052, 2010.

Vinayak, A., Mudgal, G., and Singh, G. B.: Environment persistent free radicals: Long-lived particles, in: Free Radical Biology and Environmental Toxicity, Springer, 1–19, https://doi.org/10.1007/978-3-030-83446-3, 2022.

Wan, Z., Sun, Y., Tsang, D. C., Hou, D., Cao, X., Zhang, S., Gao, B., and Ok, Y. S.: Sustainable remediation with an electroactive biochar system: mechanisms and perspectives, Green. Chem., 22, 2688–2711, https://doi.org/10.1039/D0GC00717J, 2020.

Wang, L., Zhang, L., Ristovski, Z., Zheng, X., Wang, H., Li, L., Gao, J., Salimi, F., Gao, Y., and Jing, S.: Assessing the effect of reactive oxygen species and volatile organic compound profiles coming from certain types of Chinese cooking on the toxicity of human bronchial epithelial cells, Environ. Sci. Technol., 54, 8868–8877, https://doi.org/10.1021/acs.est.9b07553, 2020.

Wang, P., Pan, B., Li, H., Huang, Y., Dong, X., Ai, F., Liu, L., Wu, M., and Xing, B.: The overlooked occurrence of environmentally persistent free radicals in an area with low-rank coal burning, Xuanwei, China, Environ. Sci. Technol., 52, 1054–1061, https://doi.org/10.1021/acs.est.7b05453, 2018.

Wang, S., Song, T., Shiraiwa, M., Song, J., Ren, H., Ren, L., Wei, L., Sun, Y., Zhang, Y., and Fu, P.: Occurrence of aerosol proteinaceous matter in urban Beijing: An investigation on composition, sources, and atmospheric processes during the "APEC Blue" period, Environ. Sci. Technol., 53, 7380–7390, https://doi.org/10.1021/acs.est.9b00726, 2019.

Wang, Y., Hopke, P. K., Sun, L., Chalupa, D. C., and Utell, M. J.: Laboratory and field testing of an automated atmospheric particle-bound reactive oxygen species sampling-analysis system, J. Toxicol., 2011, 419476, https://doi.org/10.1155/2011/419476, 2011.

Wang, Y., Arellanes, C., and Paulson, S. E.: Hydrogen peroxide associated with ambient fine-mode, diesel, and biodiesel aerosol particles in Southern California, Aerosol Sci. Tech., 46, 394–402, https://doi.org/10.1080/02786826.2011.633582, 2012.

Wang, Y., Xue, Y., Tian, H., Gao, J., Chen, Y., Zhu, C., Liu, H., Wang, K., Hua, S., Liu, S., and Shao, P.: Effectiveness

of temporary control measures for lowering $PM_{2.5}$ pollution in Beijing and the implications, Atmos. Environ., 157, 75–83, https://doi.org/10.1016/j.atmosenv.2017.03.017, 2017.

Wang, Y., Li, S., Wang, M., Sun, H., Mu, Z., Zhang, L., Li, Y., and Chen, Q.: Source apportionment of environmentally persistent free radicals (EPFRs) in $PM_{2.5}$ over Xi'an, China, Sci. Total. Environ., 689, 193–202, https://doi.org/10.1016/j.scitotenv.2019.06.424, 2019.

Wang, Y., Zhang, Y., Schauer, J. J., de Foy, B., Cai, T., and Zhang, Y.: Impacts of sources on $PM_{2.5}$ oxidation potential during and after the Asia-Pacific Economic Cooperation Conference in Huairou, Beijing, Environ. Sci. Technol., 54, 2585–2594, https://doi.org/10.1021/acs.est.9b05468, 2020.

Wang, Y., Yao, K., Fu, X. E., Zhai, X., Jin, L., and Guo, H.: Size-resolved exposure risk and subsequent role of environmentally persistent free radicals (EPFRs) from atmospheric particles, Atmos. Environ., 276, 119059, https://doi.org/10.1016/j.atmosenv.2022.119059, 2022.

Wei, J., Fang, T., Wong, C., Lakey, P. S. J., Nizkorodov, S. A., and Shiraiwa, M.: Superoxide formation from aqueous reactions of biogenic secondary organic aerosols, Environ. Sci. Technol., 55, 260–270, https://doi.org/10.1021/acs.est.0c07789, 2021.

Wu, S., Yang, B., Wang, X., Hong, H., and Yuan, C.: Diurnal variation of nitrated polycyclic aromatic hydrocarbons in PM_{10} at a roadside site in Xiamen, China, J. Environ. Sci. (China), 24, 1767–1776, https://doi.org/10.1016/S1001-0742(11)61018-8, 2012.

Xu, Y., Yang, L., Wang, X., Zheng, M., Li, C., Zhang, A., Fu, J., Yang, Y., Qin, L., Liu, X., and Liu, G.: Risk evaluation of environmentally persistent free radicals in airborne particulate matter and influence of atmospheric factors, Ecotoxicol. Environ. Saf., 196, 110571, https://doi.org/10.1016/j.ecoenv.2020.110571, 2020.

Yang, L., Liu, G., Zheng, M., Jin, R., Zhu, Q., Zhao, Y., Wu, X., and Xu, Y.: Highly elevated levels and particle-size distributions of environmentally persistent free radicals in haze-associated atmosphere, Environ. Sci. Technol., 51, 7936–7944, https://doi.org/10.1021/acs.est.7b01929, 2017.

Yang, Y., Liu, X., Qu, Y., Wang, J., An, J., Zhang, Y., and Zhang, F.: Formation mechanism of continuous extreme haze episodes in the megacity Beijing, China, in January 2013, Atmos. Res., 155, 192–203, https://doi.org/10.1016/j.atmosres.2014.11.023, 2015.

Zhang, Y., Schnelle-Kreis, J., Abbaszade, G., Zimmermann, R., Zotter, P., Shen, R., Schäfer, K., Shao, L., Prévôt, A. S. H., and Szidat, S.: Source apportionment of elemental carbon in Beijing, China: Insights from radiocarbon and organic marker measurements, Environ. Sci. Technol., 49, 8408–8415, https://doi.org/10.1021/acs.est.5b01944, 2015.

Zhao, J., Du, W., Zhang, Y., Wang, Q., Chen, C., Xu, W., Han, T., Wang, Y., Fu, P., Wang, Z., Li, Z., and Sun, Y.: Insights into aerosol chemistry during the 2015 China Victory Day parade: results from simultaneous measurements at ground level and 260 m in Beijing, Atmos. Chem. Phys., 17, 3215–3232, https://doi.org/10.5194/acp-17-3215-2017, 2017.

Zhao, K., Zhang, Y., Shang, J., Schauer, J. J., Huang, W., Tian, J., Yang, S., Fang, D., and Zhang, D.: Impact of Beijing's "Coal to Electricity" program on ambient $PM_{2.5}$ and the associated reactive oxygen species (ROS), J. Environ. Sci. (China), 133, 93–106, https://doi.org/10.1016/j.jes.2022.06.038, 2023.

Zhou, J., Zotter, P., Bruns, E. A., Stefenelli, G., Bhattu, D., Brown, S., Bertrand, A., Marchand, N., Lamkaddam, H., Slowik, J. G., Prévôt, A. S. H., Baltensperger, U., Nussbaumer, T., El-Haddad, I., and Dommen, J.: Particle-bound reactive oxygen species (PB-ROS) emissions and formation pathways in residential wood smoke under different combustion and aging conditions, Atmos. Chem. Phys., 18, 6985–7000, https://doi.org/10.5194/acp-18-6985-2018, 2018.

Zhu, K., Jia, H., Zhao, S., Xia, T., Guo, X., Wang, T., and Zhu, L.: Formation of environmentally persistent free radicals on microplastics under light irradiation, Environ. Sci. Technol., 53, 8177–8186, https://doi.org/10.1021/acs.est.9b01474, 2019.

Zhu, S., Zheng, X., Stevanovic, S., Wang, L., Wang, H., Gao, J., Xiang, Z., Ristovski, Z., Liu, J., Yu, M., Wang, L., and Chen, J.: Investigating particles, VOCs, ROS produced from mosquito-repellent incense emissions and implications in SOA formation and human health, Build. Environ., 143, 645–651, https://doi.org/10.1016/j.buildenv.2018.07.053, 2018.